Antiferromagnetism driven charge density wave in infinite-layer $NdNiO_2$ nickelates

Chen Zhang,[1,2] Xuefen Cai,[1,2] Cai-Xin Zhang,[1,2] Su-Huai Wei,[3] and Hui-Xiong Deng[1,2,*]

[1]*State Key Laboratory of Superlattices and Microstructures, Institute of Semiconductors, Chinese Academy of Sciences, Beijing 100083, China*

[2]*Center of Materials Science and Optoelectronics Engineering, University of Chinese Academy of Sciences, Beijing 100049, China*

[3]*Beijing Computational Science Research Center, Beijing 100193, China*

(Received 1 September 2023; revised 7 November 2023; accepted 18 December 2023; published 9 January 2024)

One of the central issues concerning unconventional superconductivity is the nature of the charge-density-wave (CDW) order and its implication for the pairing mechanism. Recently, a CDW order has been discovered in undoped infinite-layer $NdNiO_2$ nickelates, which cannot be explained by popular Fermi-surface-based mechanisms (such as Fermi surface nesting or strong electron-phonon coupling) due to the observed insulating behavior. In this paper, we investigate the CDW order in undoped $NdNiO_2$ using first-principles calculations. We find that the CDW order formation is independent of the Fermi surface but is strongly correlated with the intrinsic antiferromagnetic (AFM) order. We propose a CDW mechanism based on enhancement of AFM coupling induced by symmetry reduction. We demonstrate that with the loss of fourfold rotational symmetry, the Ni-$3d_{x^2-y^2}$ and Nd-$5d_{z^2}$ bonding establishes a Ni-Nd-Ni AFM superexchange channel. The AFM coupling between two adjacent Ni atoms in the same Ni-O plane is enhanced in the lower-symmetry CDW structure, making the CDW order energetically favorable and stabilized when the in-plane checkerboard AFM order is presented. Our findings suggest that AFM and lattice are strongly coupled in $NdNiO_2$ nickelates, which provides inspiration for the origin of CDW order in other strongly correlated systems and for the elucidation of the mysterious pairing mechanism.

DOI: 10.1103/PhysRevB.109.045114

Unconventional superconductors have received considerable attention for their elusive superconducting mechanism and the potential to achieve room-temperature superconductivity [1,2]. Their phase diagrams often exhibit complex and intriguing symmetry-breaking phases, such as nematic ($\mathbf{q} = 0$), spin-density-wave (SDW), and charge-density-wave (CDW; $\mathbf{q} \neq 0$) orders [3–5]. It is commonly argued that the CDW and superconducting phases share the same origin, although they often compete [5–7]. Unraveling the mechanism of CDW order may shed light on the interpretation of the origin of unconventional superconductivity.

Other than the renowned copper- and iron-based superconductors, recently discovered nickel-based superconductors provide a platform for the exploration of unconventional superconductivity [8–10]. Plenty of experiments have shown that the exotic CDW phase also presents in infinite-layer $NdNiO_2$ nickelates, while its origin is still puzzling [11–13]. Generally, among conventional superconductors exhibiting CDW order, the general origins of the CDW phase mainly include Fermi surface nesting [14,15], strong electron-phonon coupling [16,17], and van Hove singularity [18], all of which can be attributed to the energy lowering of electrons near the Fermi surface. However, none of these mechanisms can account for the formation of the CDW phase in undoped $NdNiO_2$. From the experimental point of view, the CDW order of $NdNiO_2$ is found to be strongest when undoped [11–13], when the resistivity shows insulating behaviors [19,20]; thus, the existence of a Fermi surface in $NdNiO_2$ is now highly questionable. Additionally, resonant inelastic x-ray scattering (RIXS) measurements suggest the strong involvement of empty Nd-$5d_{z^2}$ orbitals during CDW phase formation [11–13], likewise posing a great challenge to the Fermi-surface-based CDW mechanism. Theoretically, density functional theory (DFT) calculations with the Fermi-surface-based mechanism also failed to predict the electronic and structural instability of the high-symmetry structure [21]. Therefore, it is of great interest to propose a fundamental understanding of the origin of the CDW phase in $NdNiO_2$.

In this paper, we use first-principles calculations to investigate the formation and origin of the CDW phase in undoped $NdNiO_2$. We find that the CDW order in undoped $NdNiO_2$ is indeed irrelevant to the Fermi surface but is instead heavily dependent on the intrinsic antiferromagnetic (AFM) order. The strong dependence between the CDW and AFM orders has inspired us to propose a CDW mechanism based on symmetry-reduction-induced enhancement of AFM coupling. In the CDW phase, with the loss of fourfold rotational symmetry, a Ni-Nd-Ni AFM superexchange channel between the adjacent Ni atoms in the same Ni-O plane is established through the coupling between the Ni-$3d_{x^2-y^2}$ and Nd-$5d_{z^2}$ orbitals. The AFM coupling between two in-plane neighboring Ni atoms is thus enhanced, leading to a significant energy gain when the in-plane checkerboard AFM order is presented. In summary, our findings suggest a strong coupling between AFM and lattice relaxation in $NdNiO_2$. This implies that both

*hxdeng@semi.ac.cn

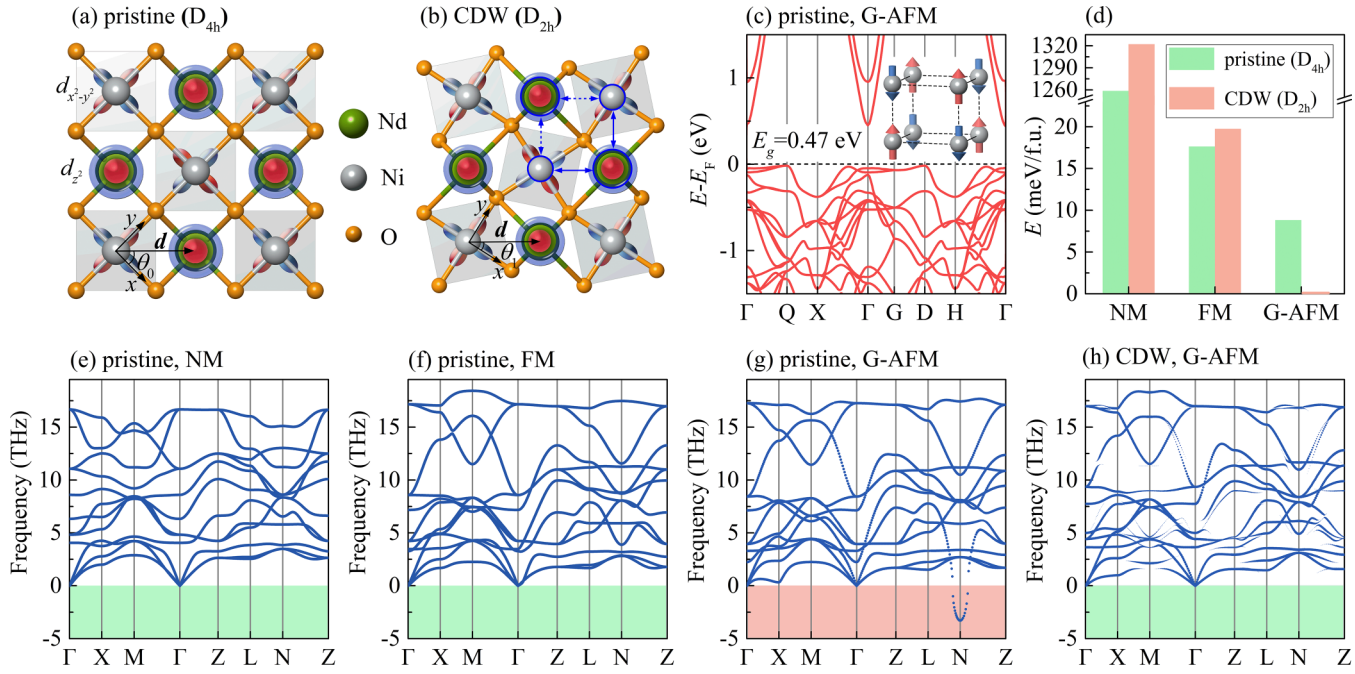

FIG. 1. The atomic structure of (a) the D_{4h} pristine phase and (b) the D_{2h} charge-density wave (CDW) phase. The green, gray, and yellow balls represent Nd, Ni, and O atoms, respectively. In (a) and (b), **d** is the interatomic vector pointing from Ni to Nd, and θ_0 and θ_1 are the corresponding azimuthal angles. The blue arrows in (b) indicate possible Ni-Nd-Ni superexchange channels. (c) The band structure of the D_{4h} pristine structure with the G-antiferromagnetic (AFM) order. Since the Kramers' degeneracy still holds, only the spin-up part is presented. The inset in (c) shows the spin arrangement of the G-AFM order. (d) The total energy of different structures in different magnetic orders. All energies are referenced to the total energy of the D_{2h} CDW structure with the G-AFM order. Details about the different cell sizes used for calculating total energy refer to Fig. S3 in the SM [27]. And the unfolded phonon spectrum of (e) the pristine structure with nonmagnetic (NM) order, (f) the pristine structure with ferromagnetic (FM) order, (g) the pristine structure with the G-AFM order, and (h) the CDW structure with the G-AFM order.

lattice dynamics and AFM should be vital for the mechanism of high-temperature superconductivity.

Our calculations employ DFT as implemented in VASP [22,23], and the Perdew-Burke-Ernzerhof approximation [24] is utilized for the exchange-correlation functional. For Nd atoms, the $4f^3$ electrons are assigned to a nonmagnetic (NM) core to ensure the correct occupancy of the f orbitals. The cutoff energy of the plane-wave basis is set to 400 eV, the energy convergence threshold is set to 10^{-6} eV, and a Γ-centered k-point mesh with $2\pi \times 0.03$ Å^{-1} spacing is used for Brillouin zone sampling. All original static structures were relaxed to their optimum configurations so that Hellmann-Feynman forces on each atom reach <0.01 eV/Å. All phonon spectra were determined using the finite-displacement method as implemented in the PHONOPY package [25], and $2\sqrt{2}\times2\sqrt{2}\times4$ supercells with 128 atoms included are constructed for phonon calculations. To test the robustness of the CDW order under different correlation strengths, based on the previous work [26], we applied an on-site Coulomb repulsion U with values of 4, 6, and 8 eV on $3d$ orbitals of Ni atoms and found that our conclusion is not affected by the U parameter (see Figs. S1 and S2 in the Supplemental Material (SM) [27]). Therefore, we present only the results for $U_{\mathrm{Ni}-3d} = 8$ eV. With $NdNiO_2$ being a structural and electronic analog to the $CaCuO_2$ cuprates, its pristine structure adopts a D_{4h} crystallographic point group, and there is a fourfold rotational axis through the Nd atoms perpendicular to the Ni-O plane [Fig. 1(a)]. The stable Ni^{1+} is in the $3d^9$ configuration, and the highest-lying $d_{x^2-y^2}$ orbital is half-filled [28,29], leaving each Ni atom with a calculated magnetic moment of about 1 μ_B, in agreement with the previous DFT results [26].

In addition, we use the cluster expansion method [30] to explore the changes in magnetic exchange interactions before and after the formation of the CDW order. The total energies of different magnetic configurations are expanded by $E(\sigma) = N\sum_f J_f D_f \bar{\pi}_f(\sigma)$, where $E(\sigma)$ is the total energy of the configuration σ with N sites. For a specific cluster figure f, D_f is its degeneracy, and $\bar{\pi}_f(\sigma)$ is the correlation function defined as the lattice-averaged product of spins. For convenience, we assign different spin orientations as ±1. The multispin effective cluster interaction parameters J_f are derived by fitting the total energies of $n+1$ configurations (where n is the number of considered clusters) with the smallest cell size. We gradually increase the number of clusters used for fitting based on the effective cluster interaction selection rule until the predicted ground state and the ground state from DFT calculations converge, while the cross-validation score is kept <2 meV/site [30].

The CDW order reduces the total energy of the system by reconstructing the lattice and associated electrons and is usually evidenced by the imaginary frequency at $\mathbf{q} \neq 0$ in the phonon spectrum of the high-symmetry structure [31]. Therefore, to investigate the potential CDW order in undoped

$NdNiO_2$, we calculated the phonon spectrum of different structures with different magnetic orders in Figs. 1(e)–1(h). When the magnetic order is set to be NM [Fig. 1(e)] or ferromagnetic [FM, Fig. 1(f)], no imaginary frequency is presented, and the D_{4h} pristine structure is kinetically stable, consistent with previous DFT results [21].

However, when the magnetic order on the Ni atoms is set to more stable G-AFM [26] [with spins in antiparallel alignment both in-plane and out-of-plane, inset in Fig. 1(c)], an imaginary frequency appears at the N (π, π, π) point in its phonon spectrum [Fig. 1(g)], and the corresponding vibrational mode corresponds to the B_{3g} rotational (Ni-O bond bending) mode of the Ni-O plaquette. After O atoms are displaced according to the relevant phonon mode and a full relaxation is performed, we have obtained a lower-symmetry CDW structure with lower energy [$\sim$11 meV/f.u., Figs. 1(b) and 1(d)]. In the relaxed CDW structure, each Ni-O plaquette rotates roughly $\theta_0 - \theta_1 = 4.47^\circ$ around the rotation axis perpendicular to the Ni-O plane. Now the original fourfold rotational axis through the Nd atoms disappears, and the symmetry of the system is reduced to D_{2h}. The phonon spectrum calculated from the CDW structure no longer shows the presence of imaginary frequencies [Fig. 1(h)], indicating the kinetic stability of the D_{2h} CDW structure. In contrast to the G-AFM case, for the NM or FM spin order, the D_{2h} CDW structure has a higher total energy than the D_{4h} pristine structure [Fig. 1(d)], thus is energetically disfavored, suggesting that this D_{2h} CDW order formation could not be related to the NM or FM but to the G-AFM spin order.

It is worth noting that the undoped $NdNiO_2$ with the G-AFM order is calculated to be an insulator with a band gap of 0.47 eV [Fig. 1(c)]. Despite the absence of the Fermi surface in the G-AFM state, the D_{2h} CDW structure remains energetically more stable than the D_{4h} pristine structure [Fig. 1(d)], indicating that the CDW order formation does not depend on the presence of the Fermi surface. Thus, the Fermi-surface-based CDW mechanism (such as Fermi surface nesting or strong electron-phonon coupling) should no longer hold for undoped $NdNiO_2$. We note that the in-plane ordering wave vector of our proposed CDW order at the N point (π, π) [Fig. 1(g)] differs from the experimentally observed $(\frac{1}{3}, 0)$. This deviation could be attributed to the absence of AFM long-range order in the experimental samples [32]. However, since both CDW orders share the same characteristic of breaking fourfold rotational symmetry, they could arise from the same mechanism.

To further understand the role of the G-AFM order in the CDW order formation, we have performed cluster expansions to determine the magnetic interaction parameters in the D_{4h} pristine and D_{2h} CDW structures, respectively. In the absence of an external magnetic field, the total energy remains unchanged after all spins flip; thus, the three-spin interaction terms should be zero, and only the two- and four-spin interaction terms remain, consistent with the t/U expansion of the Hubbard model [33,34]. Clusters containing pairs up to the fifth nearest neighbors and quadruplets up to the fourth nearest neighbors are included when performing cluster expansion. The corresponding effective pair interaction parameters (J_p) obtained by fitting the total energies are displayed in Fig. 2. It can be observed from Fig. 2 that the key figure for the

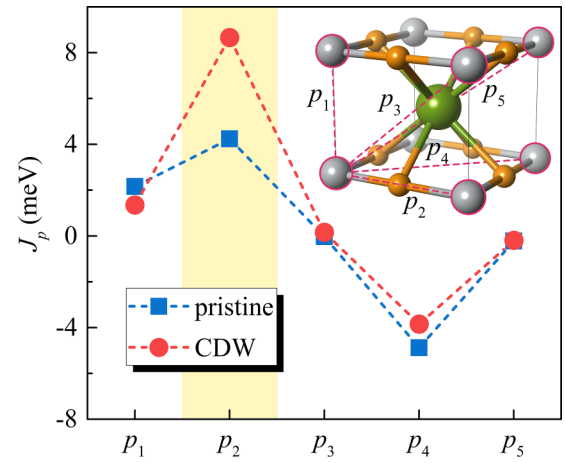

FIG. 2. The fitted effective pair interaction parameters (J_p) under D_{4h} pristine and D_{2h} charge-density-wave (CDW) structures. The inset shows the definition of pair figures up to the fifth nearest neighbors.

CDW order formation should be p_2, as it is the only pair whose interaction parameter undergoes a significant change after the formation of the CDW order. The figure p_2 features the exchange interaction between the two adjacent Ni atoms in the same Ni-O plane (inset in Fig. 2). In the D_{4h} pristine structure, due to the established Ni-O-Ni AFM superexchange channel, the magnetic moments on the two in-plane adjacent Ni atoms favor an antiparallel alignment $J_{p2} > 0$, which is consistent with the previous DFT calculations [26]. After the CDW order is formed, J_{p2} increases significantly, and the AFM coupling between two in-plane neighboring Ni atoms is enhanced (Fig. 2), thus causing the D_{2h} CDW structure to be energetically more stable than the D_{4h} pristine structure when the in-plane checkerboard AFM order [inset in Fig. 1(c)] is presented.

However, this leads to another question: Why is the J_{p2} parameter of AFM interaction strengthened? It would not arise from the conventional Ni-O-Ni channel because, according to the Goodenough-Kanamori-Anderson rules [35], as the bond angle between Ni-O-Ni deviates from 180° in the CDW structure, the AFM coupling between two adjacent Ni atoms should be weakened rather than strengthened. Due to the confirmed significant role of Nd-$5d_{z^2}$ orbitals in the CDW formation by RIXS measurements [11–13], it is worthwhile to analyze this orbital from a more fundamental perspective. The coupling strength between the Ni-$3d_{x^2-y^2}$ and Nd-$5d_{z^2}$ orbitals is determined by the interatomic Slater-Koster two-center integral, which can be written as $t_{x^2-y^2,z^2} = \frac{\sqrt{3}}{2}(l^2 - m^2)[n^2 - \frac{1}{2}(l^2 + m^2)]V_{dd\sigma} + \sqrt{3}n^2(l^2 - m^2)V_{dd\pi} + \frac{\sqrt{3}}{4}(1 + n^2)(l^2 - m^2)V_{dd\delta}$. Here, $V_{dd\sigma}$, $V_{dd\pi}$, and $V_{dd\delta}$ are the radial integrals when forming σ, π, and δ bonds, respectively, and $l = \mathbf{d} \cdot \mathbf{x}/|\mathbf{d}|$, $m = \mathbf{d} \cdot \mathbf{y}/|\mathbf{d}|$, and $n = \mathbf{d} \cdot \mathbf{z}/|\mathbf{d}|$ are the direction cosines [36], where $\mathbf{d}$ is the interatomic vector pointing from Ni to Nd. Obviously, $l = \cos\theta\sin\varphi$ and $m = \sin\theta\sin\varphi$, where θ and φ are the azimuthal and polar angles of the interatomic Ni-Nd vector, respectively [Figs. 1(a) and 1(b)]. In the high-symmetry pristine structure with point group of D_{4h}, $\theta_0 = 45^\circ$ is ensured by the

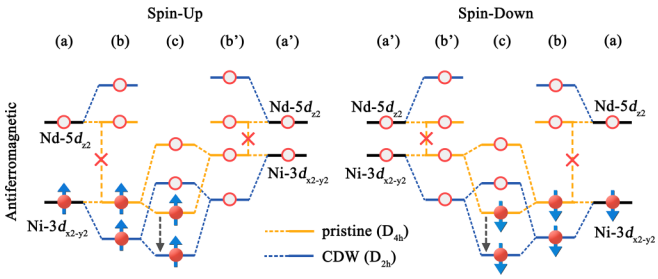

FIG. 3. The schematic of orbital coupling in the D_{4h} pristine structure and in the D_{2h} charge-density-wave (CDW) structure, respectively, when in the antiferromagnetic (AFM) alignment. The red × denotes the forbidden coupling between the Ni-3$d_{x^2-y^2}$ and Nd-5d_{z^2} orbitals.

fourfold rotational axis through the Nd atom [Fig. 1(a)], then $l = m$, $t_{x^2-y^2,z^2} = 0$; thus, the coupling between Ni-3$d_{x^2-y^2}$ and Nd-5d_{z^2} orbitals is forbidden (Fig. 3). However, in the lower-symmetry CDW structure with point group of D_{2h}, as the original fourfold rotation operation vanishes, $\theta_1 = 40.53^\circ \neq 45^\circ$ [Fig. 1(b)], $l \neq m$, $t_{x^2-y^2,z^2} \neq 0$, Ni-3$d_{x^2-y^2}$ and Nd-5d_{z^2} orbitals begin to couple, thus establishing a Ni-Nd-Ni superexchange channel [blue arrows in Fig. 1(b)]. Because the Ni-3$d_{x^2-y^2}$ majority spin levels are fully occupied, this superexchange channel still should be of AFM type based on magnetic coupling model [37].

Furthermore, in Fig. 3, we provide a comprehensive illustration of the stabilization process of the D_{2h} CDW structure through this Ni-Nd-Ni superexchange channel by band coupling model. First, from (a) to (b) or (a′) to (b′) in both spin channels, the electronic energy can be lowered by direct coupling between the Ni-3$d_{x^2-y^2}$ and Nd-5d_{z^2} orbitals by pushing down the occupied Ni-3$d_{x^2-y^2}$ orbitals. Then from (b) to (c) or (b′) to (c) in both spin channels, in the AFM alignment, the electronic energy can be further lowered by the coupling between the occupied Ni-3$d_{x^2-y^2}$ from one Ni atom and the unoccupied Ni-3$d_{x^2-y^2}$ orbitals from the neighboring Ni atoms. Thus, compared with the absence of coupling between the Ni-3$d_{x^2-y^2}$ and Nd-5d_{z^2} orbitals in the D_{4h} pristine structure, a significant energy gain is obtained through the Ni-Nd-Ni superexchange channel, causing the J_{p2} interaction between the two neighboring Ni atoms in the same Ni-O plane to be greatly reinforced and ultimately stabilizing the D_{2h} CDW structure in the G-AFM order.

In conclusion, we have investigated the CDW order in undoped infinite-layer $NdNiO_2$ nickelates and proposed a Fermi-surface-independent CDW formation mechanism. We have proposed a CDW order in $NdNiO_2$ that is free from the Fermi surface but strongly correlated with the intrinsic AFM order. We suggest that, in the CDW structure, where the fourfold rotational symmetry vanishes, the Ni-3$d_{x^2-y^2}$ orbitals start to couple with the Nd-5d_{z^2} orbitals to establish a Ni-Nd-Ni AFM superexchange channel. The AFM coupling between two in-plane adjacent Ni atoms is strengthened, leading to a significant energy gain when the in-plane checkerboard AFM order is presented. This proposed CDW mechanism ought to offer some inspiration for the origin of CDW transition in other AFM-rooted strongly correlated systems.

This paper was supported by the National Natural Science Foundation of China (Grants No. 61922077, No. 11874347, No. 11991060, No. 12088101, No. 61927901, and No. U2230402), the National Key Research and Development Program of China (Grants No. 2018YFB2200100 and No. 2020YFB1506400), the Strategic Priority Research Program of the Chinese Academy of Sciences (Grant No. XDB0460000), and the CAS Project for Young Scientists in Basic Research (No. YSBR-026). H.-X.D. was also supported by the Youth Innovation Promotion Association of Chinese Academy of Sciences (Grant No. Y2021042).

[1] J. G. Bednorz and K. A. Müller, Possible high T_c superconductivity in the Ba-La-Cu-O system, Z. Phys. B: Condens. Matter **64**, 189 (1986).

[2] N. Singh, Leading theories of the cuprate superconductivity: A critique, Physica C **580**, 1353782 (2021).

[3] V. J. Emery, S. A. Kivelson, and J. M. Tranquada, Stripe phases in high-temperature superconductors, Proc. Natl. Acad. Sci. USA **96**, 8814 (1999).

[4] E. Fradkin, S. A. Kivelson, and J. M. Tranquada, Colloquium: Theory of intertwined orders in high temperature superconductors, Rev. Mod. Phys. **87**, 457 (2015).

[5] A. M. Gabovich, A. I. Voitenko, and M. Ausloos, Charge-and spin-density waves in existing superconductors: Competition between Cooper pairing and Peierls or excitonic instabilities, Phys. Rep. **367**, 583 (2002).

[6] E. Demler, W. Hanke, and S.-C. Zhang, $SO(5)$ theory of antiferromagnetism and superconductivity, Rev. Mod. Phys. **76**, 909 (2004).

[7] C.-W. Chen, J. Choe, and E. Morosan, Charge density waves in strongly correlated electron systems, Rep. Prog. Phys. **79**, 084505 (2016).

[8] D. Li, K. Lee, B. Y. Wang, M. Osada, S. Crossley, H. R. Lee, Y. Cui, Y. Hikita, and H. Y. Hwang, Superconductivity in an infinite-layer nickelate, Nature (London) **572**, 624 (2019).

[9] D. Li, B. Y. Wang, K. Lee, S. P. Harvey, M. Osada, B. H. Goodge, L. F. Kourkoutis, and H. Y. Hwang, Superconducting dome in $Nd_{1-x}Sr_xNiO_2$ infinite layer films, Phys. Rev. Lett. **125**, 027001 (2020).

[10] S. Zeng, C. S. Tang, X. Yin, C. Li, M. Li, Z. Huang, J. Hu, W. Liu, G. J. Omar, H. Jani *et al.*, Phase diagram and superconducting dome of infinite-layer $Nd_{1-x}Sr_xNiO_2$ thin films, Phys. Rev. Lett. **125**, 147003 (2020).

[11] M. Rossi, M. Osada, J. Choi, S. Agrestini, D. Jost, Y. Lee, H. Lu, B. Y. Wang, K. Lee, A. Nag *et al.*, A broken translational symmetry state in an infinite-layer nickelate, Nat. Phys. **18**, 869 (2022).

[12] C. C. Tam, J. Choi, X. Ding, S. Agrestini, A. Nag, M. Wu, B. Huang, H. Luo, P. Gao, M. Garcia-Fernandez *et al.*, Charge density waves in infinite-layer $NdNiO_2$ nickelates, Nat. Mater. **21**, 1116 (2022).

[13] G. Krieger, L. Martinelli, S. Zeng, L. E. Chow, K. Kummer, R. Arpaia, M. Moretti Sala, N. B. Brookes, A. Ariando, N. Viart

et al., Charge and spin order dichotomy in $NdNiO_2$ driven by the capping layer, Phys. Rev. Lett. **129**, 027002 (2022).

[14] P. Aebi, T. Pillo, H. Berger, and F. Lévy, On the search for Fermi surface nesting in quasi-2D materials, J. Electron Spectrosc. Relat. Phenom. **117–118**, 433 (2001).

[15] M. D. Johannes and I. I. Mazin, Fermi surface nesting and the origin of charge density waves in metals, Phys. Rev. B **77**, 165135 (2008).

[16] C. M. Varma and A. L. Simons, Strong-coupling theory of charge-density-wave transitions, Phys. Rev. Lett. **51**, 138 (1983).

[17] Y. Liu, D. F. Shao, L. J. Li, W. J. Lu, X. D. Zhu, P. Tong, R. C. Xiao, L. S. Ling, C. Y. Xi, L. Pi *et al.*, Nature of charge density waves and superconductivity in $1T$–$TaSe_{2-x}Te_x$, Phys. Rev. B **94**, 045131 (2016).

[18] T. M. Rice and G. K. Scott, New mechanism for a charge-density-wave instability, Phys. Rev. Lett. **35**, 120 (1975).

[19] Q. Li, C. He, J. Si, X. Zhu, Y. Zhang, and H.-H. Wen, Absence of superconductivity in bulk $Nd_{1-x}Sr_xNiO_2$, Commun. Mater. **1**, 16 (2020).

[20] B. X. Wang, H. Zheng, E. Krivyakina, O. Chmaissem, P. P. Lopes, J. W. Lynn, L. C. Gallington, Y. Ren, S. Rosenkranz, J. F. Mitchell *et al.*, Synthesis and characterization of bulk $Nd_{1-x}Sr_xNiO_2$ and $Nd_{1-x}Sr_xNiO_3$, Phys. Rev. Mater. **4**, 084409 (2020).

[21] X. Sui, J. Wang, C. Chen, X. Ding, K.-J. Zhou, C. Cao, L. Qiao, H. Lin, and B. Huang, Hole doping dependent electronic instability and electron-phonon coupling in infinite-layer nickelates, Phys. Rev. B **107**, 075159 (2023).

[22] G. Kresse and J. Furthmüller, Efficiency of *ab-initio* total energy calculations for metals and semiconductors using a plane-wave basis set, Comput. Mater. Sci. **6**, 15 (1996).

[23] G. Kresse and J. Furthmüller, Efficient iterative schemes for *ab initio* total-energy calculations using a plane-wave basis set, Phys. Rev. B **54**, 11169 (1996).

[24] J. P. Perdew, K. Burke, and M. Ernzerhof, Generalized gradient approximation made simple, Phys. Rev. Lett. **77**, 3865 (1996).

[25] A. Togo, First-principles phonon calculations with PHONOPY and PHONO3PY, J. Phys. Soc. Jpn. **92**, 012001 (2023).

[26] Z. Liu, Z. Ren, W. Zhu, Z. Wang, and J. Yang, Electronic and magnetic structure of infinite-layer $NdNiO_2$: Trace of antiferromagnetic metal, npj Quantum Mater. **5**, 31 (2020).

[27] See Supplemental Material at http://link.aps.org/supplemental/10.1103/PhysRevB.109.045114 for results with different U parameters, and cell size descriptions for total energy calculations.

[28] H. Sakakibara, H. Usui, K. Suzuki, T. Kotani, H. Aoki, and K. Kuroki, Model construction and a possibility of cupratelike pairing in a new d^9 nickelate superconductor (Nd, Sr)NiO_2, Phys. Rev. Lett. **125**, 077003 (2020).

[29] A. S. Botana and M. R. Norman, Similarities and differences between $LaNiO_2$ and $CaCuO_2$ and implications for superconductivity, Phys. Rev. X **10**, 011024 (2020).

[30] A. van de Walle and G. Ceder, Automating first-principles phase diagram calculations, J. Phase Equilib. **23**, 348 (2002).

[31] X. Zhu, Y. Cao, J. Zhang, E. W. Plummer, and J. Guo, Classification of charge density waves based on their nature, Proc. Natl. Acad. Sci. USA **112**, 2367 (2015).

[32] M. A. Hayward and M. J. Rosseinsky, Synthesis of the infinite layer Ni(I) phase $NdNiO_{2+x}$ by low temperature reduction of $NdNiO_3$ with sodium hydride, Solid State Sci. **5**, 839 (2003).

[33] A. H. MacDonald, S. M. Girvin, and D. Yoshioka, t/U expansion for the Hubbard model, Phys. Rev. B **37**, 9753 (1988).

[34] M. Hoffmann and S. Blügel, Systematic derivation of realistic spin models for beyond-Heisenberg solids, Phys. Rev. B **101**, 024418 (2020).

[35] E. Koch, Exchange mechanisms, in *Correlated Electrons: From Models to Materials*, edited by E. Pavarini, E. Koch, F. Anders, and M. Jarrell (Forschungszentrum Jülich GmbH, Jülich, 2012), Vol. 2, Chap. 7.

[36] E. Pavarini, Crystal-field theory, tight-binding method and Jahn-Teller effect, in *Correlated Electrons: From Models to Materials*, edited by E. Pavarini, E. Koch, F. Anders, and M. Jarrell (Forschungszentrum Jülich GmbH, Jülich, 2012), Vol. 2, Chap. 6.

[37] G. M. Dalpian, S.-H. Wei, X. G. Gong, A. J. R. da Silva, and A. Fazzio, Phenomenological band structure model of magnetic coupling in semiconductors, Solid State Commun. **138**, 353 (2006).